Transgenic expression of human matrix metalloproteinase-9 augments monocrotaline-induced pulmonary arterial hypertension in mice

Joseph George and Jeanine D'Armiento

Objectives **Pulmonary arterial hypertension (PAH) is characterized by intimal lesions, right ventricular hypertrophy, and adventitial thickening of pulmonary arteries with progressive pulmonary hypertension. This investigation was aimed to examine the effects of transgenic expression of human matrix metalloproteinase-9 (MMP-9) in the pathogenesis of PAH.**

Methods **PAH was induced using serial subcutaneous administration of monocrotaline (MCT). Right ventricular pressure was measured through the right jugular vein using a 1.4F Millar Mikro-tip catheter-transducer. Zymography, western blotting, and quantitative reverse transcription PCR (qRT-PCR) were carried out for MMP-9. Immunohistochemistry was performed for α-smooth muscle actin (α-SMA) and Mac-3 antigen.**

Results **Measurement of right ventricular pressure demonstrated 2.5-fold and 3.7-fold elevation after the administration of MCT in wild-type and MMP-9 transgenic mice, respectively. Zymography, western blotting, and qRT-PCR depicted increased activity and expression of MMP-9 after treatment with MCT, which were augmented in transgenic mice. There was marked pulmonary inflammation with extensive infiltration of mononuclear cells, which was more intense in MMP-9 transgenic mice. SMA and Mac-3 staining demonstrated hypertrophy of pulmonary arteries with occlusion of precapillary vessels and extensive infiltration of macrophages, respectively. All these changes were aggravated in MCT-treated MMP-9 transgenic mice when compared to normal littermates.**

Conclusion **Our study demonstrated that the MCT-induced PAH in mouse is a reproducible and potentially valuable animal model for the human disease. Our results further demonstrated that MMP-9 plays a significant role in the pathogenesis of PAH and effective blocking of MMP-9 could provide an option in the therapeutic intervention of human PAH. *J Hypertens* 29:299–308 © 2011 Wolters Kluwer Health | Lippincott Williams & Wilkins.**

Journal of Hypertension 2011, **29**:299–308

Keywords: matrix metalloproteinases, MMP-9 transgene, monocrotaline, pulmonary arterial hypertension, pulmonary occlusion, right ventricular pressure

Abbreviations: α-SMA, α-smooth muscle actin; AEC, 3-amino-9-ethylcarbazole; ApoE, apolipoprotein E; Mac-3, Macrophage-3; MCT, monocrotaline; MMPs, matrix metalloproteinases; PAH, pulmonary arterial hypertension; PVDF, polyvinylidene fluoride; qRT-PCR, quantitative reverse transcription polymerase chain reaction

Division of Molecular Medicine, Department of Medicine, Columbia University, New York, New York, USA

Correspondence to Joseph George, PhD, Department of Medicine, Division of Liver Diseases, Mount Sinai School of Medicine, 1425 Madison Avenue, New York, NY 10029, USA
Tel: +1 212 659 9217; fax: +1 212 849 2574;
e-mails: jgeorge40@hotmail.com, joseph.george@mssm.edu

Received 21 April 2010 **Revised** 14 September 2010
Accepted 15 September 2010

Introduction

Pulmonary arterial hypertension (PAH) is a debilitating and life-threatening disease often affecting young people [1,2]. PAH is characterized by intimal lesions, medial hypertrophy, and adventitial thickening of precapillary pulmonary arteries with progressive pulmonary hypertension [3,4]. Increased vasomotor tone and chronic remodeling of the precapillary resistance vessels, including marked vascular smooth muscle cell growth, are the underlying pathogenetic mechanisms in this disease [5,6]. Increased collagen depositions in the inner pulmonary arterial wall and systemic sclerosis are certain characteristic features of PAH [7,8]. The molecular mechanisms involved in the regulation of collagen deposition during pulmonary hypertension are poorly understood.

Monocrotaline (MCT) is a pyrrolizidine alkaloid extracted from the seeds and leaves of the plant *Crotalaria spectabilis*. The metabolic products of MCT are both hepatotoxic and pneumotoxic in several species [9]. The disorder of MCT-induced lung injury in rats includes interstitial edema, inflammation, hemorrhage, and fibrosis, accompanied by medial hypertrophy of the pulmonary arteries, pulmonary hypertension, and right ventricular hypertrophy [10]. MCT causes pulmonary arterial endothelial cell injury and subsequent pulmonary artery smooth muscle hypertrophy with persistent severe pulmonary hypertension after one injection in rats [11]. A dose of MCT as low as 2.4 mg/kg body weight could induce pulmonary toxicity in rats after a 6-week regimen [12]. However, mice require a 10-fold higher dosage to produce cardiopulmonary changes after 6 weeks of treatment with MCT at doses of 24 mg/kg body weight [12]. Qualitative and quantitative biochemical and morphological differences were also reported between mice and rats with respect to MCT pneumotoxicity [12].

0263-6352 © 2011 Wolters Kluwer Health | Lippincott Williams & Wilkins DOI:10.1097/HJH.0b013e328340a0e4

Matrix metalloproteinases (MMPs) are involved in the pathogenesis of various lung diseases such as lung cancer, bronchial asthma, chronic obstructive pulmonary disease, acute lung injury, pulmonary hypertension, and interstitial lung diseases [13–15]. MMPs play a significant role in the remodeling of vascular tissue during the pathogenesis of PAH [16,17]. An increase in the expression of MMP-2 and MMP-9 has been reported in MCT-induced experimental pulmonary hypertension in rats [18]. However, the exact role of MMPs in the pathogenesis of pulmonary arterial hypertension is not known.

The purpose of this investigation was first to develop a suitable mouse model for PAH using MCT and second to study the effects of transgenic expression of human MMP-9 in the pathogenesis of PAH in a mouse model.

Methods

Animals

All animal experiments were carried out with the *Guide for the Care and Use of Laboratory Animals* published by the US National Institutes of Health (NIH Publication No. 85-23, revised 1996) and also in compliance with our Institutional Animal Care and Use Committee. A MMP-9 transgenic mouse was generated by ligating the 2.4 kb cDNA of human proMMP-9 (a gift from Dr Goldberg, Washington University) between two *Xba*I sites under the control of human scavenger receptor-enhancer promoter A. This promoter allows specific expression of the transgene in tissue macrophages. The MMP-9 cDNA construct was microinjected into fertilized mouse eggs from (C57BL/6J × CBA/J) × (C57BL/6J × CBA/J) genetic background. Newborn mice that express the transgene were established through Southern blotting and PCR analysis. Mice were then backcrossed into the C57B6 strain. Age-matched littermates that do not express the transgene were used as control mice.

Induction of pulmonary arterial hypertension

Monocrotaline (Sigma, St Louis, Missouri, USA) powder was dissolved in 0.1 N HCl, adjusted the pH to 7.4 with 0.1 N NaOH and sterilized through 0.22 μm disc filter. Male mice at 3 months of age weighing around 25 g were used for the studies. PAH was induced with serial subcutaneous injections of MCT in doses of 60 mg/100 g body weight once a week for 8 consecutive weeks. The injections were given to MMP-9 transgenic and parental wild-type mice. Control animals from both group received similar injections (vehicle) without MCT. A total of six animals were studied in each group. All the animals were maintained with commercial mice feed and water available *ad libitum*. The animals were studied on the eighth day of the last MCT administration.

Measurement of right ventricular pressure

The right ventricular systolic pressure was measured in wild-type and MMP-9 transgenic mice after the induction of PAH with MCT. Right ventricular pressure was also measured in both groups of control mice. The animals were anesthetized with intraperitoneal injections of Avertin (tribromoethanol) at a dose of 0.15 ml/10 g body weight and then ventilated with a rodent ventilator (Harvard Apparatus, Holiston, Massachusetts, USA) with airflow of 1 ml/100 g body weight and a frequency of 60 s^{-1} after tracheotomy. Anesthesia was maintained with isoflurane. A superficial incision was made on the right ventral of the neck, and a portion of the right jugular vein was carefully exposed without bleeding. The distal portion of the jugular vein was ligated using a suture thread, and the proximal part was positioned with a small vessel clamp. A small incision was made on the jugular vein between the ligation and the vessel clamp, and a 1.4F Millar Mikro-tip catheter-transducer (Model SPR-671, Millar Instruments, Houston, Texas, USA) was inserted carefully. The catheter-transducer was secured with another suture thread, and the vessel clamp was removed. Then the catheter-transducer was slowly advanced through the jugular vein into the right atrium and then into the right ventricle. Progress of the catheter-transducer movement was monitored, and the pressure waveform was recorded using PowerLab (ADInstruments, Colorado Springs, Colorado, USA).

Gelatin zymography for matrix metalloproteinase-9

The activity of MMP-9 and MMP-2 in the lung tissue of wild-type and MMP-9 transgenic mice was assayed using gelatin zymography [19]. About 100 mg of fresh lung tissue was homogenized in 1 ml of Tris–HCl buffer (50 mmol/l Tris, 150 mmol/l NaCl and 1% Triton X-100 and the pH was adjusted to 8.00 with concentrated HCl). The homogenate was centrifuged at 13 000 rpm for 30 min at 4°C, and the supernatant was collected. After equalizing the protein concentration, about 30 μg protein was resolved on a 10% SDS-PAGE prepared with 0.1% gelatin under nonreducing conditions. The gels were washed twice (30 min/wash) in 2.5% Triton X-100 at room temperature and then incubated overnight at 37°C in 50 mmol/l Tris–HCl buffer containing 10 mmol/l calcium chloride (pH 7.6). The gels were stained with Coomassie brilliant blue R-250 for 30 min and then destained. MMP-9 and MMP-2 activity was visualized as clear transparent bands and photographed. The clear bands were quantified using Gel-Pro analyzer software (Media Cybernetics, Silver Spring, Maryland, USA).

Western blotting for matrix metalloproteinase-9

About 100 μg of protein prepared as above was denatured and resolved on a 7.5% SDS-PAGE. The separated proteins were electroblotted to an activated polyvinylidene fluoride (PVDF) membranes (Millipore, Bedford, MA, USA) and blocked with 5% milk. The membranes were incubated overnight on a rocker at 4°C with MMP-9 antibody (Santa Cruz Biotechnology, Santa Cruz, California, USA), which reacts with mouse and human

followed by incubation with horseradish peroxidase (HRP) conjugated respective secondary antibody (Biomeda, Foster City, California, USA) at room temperature for 2 h. The membranes were washed, treated with enhanced chemiluminescence reagent (Amersham, UK), exposed to BioMax XAR autoradiography film (Kodak, New Haven, Connecticut, USA), and developed. The membranes were reprobed for β-actin content to demonstrate uniform loading of protein in each lane.

Quantitative real-time RT-PCR for matrix metalloproteinase-9

Control and MCT-treated mice lung tissues were instantly frozen in liquid nitrogen and stored at −80°C. Total cellular RNA was isolated using the RNeasy kit (Qiagen, Valencia, California, USA). The quality of the isolated RNA was validated using UV-spectrometry as well as on agarose gel. Mouse and human MMP-9 primers were designed using Primer 3 software and further evaluated. We used the following primer sequences for quantitative real-time RT-PCR analysis for mouse MMP-9 (NM_013599, forward: 5′-CGT CGT GAT CCC CAC TTA CT-3′ and reverse: 5′-AAC ACA CAG GGT TTG CCT TC-3′) and transgenic human MMP-9 (NM_004994, forward: 5′-TTG ACA GCG ACA AGA AGT GG-3′ and reverse: 5′-GCC ATT CAC GTC GTC CTT AT-3′) genes. Real-time RT-PCR was carried out using a one-step RT-PCR kit with SYBR green (Bio-Rad, Hercules, California, USA) on a real-time PCR machine (iCycler iQ5; Bio-Rad) with the following reaction conditions: cDNA synthesis, 10 min at 50°C; reverse transcriptase inactivation at 95°C for 5 min; PCR cycling and detection at 95°C for 10 s; and data collection at 56°C for 30 s. Approximately 100 ng of total isolated RNA was transcribed.

Hematoxylin and eosin and Masson's trichrome staining

The pathogenesis of MCT-induced PAH and the effects of human MMP-9 transgene were evaluated through hematoxylin and eosin (H&E) as well as Masson's trichrome staining. The lungs were aerated and perfused with 3% paraformaldehyde for 20 min before fixing in 10% phosphate-buffered formalin. Two to three lobes of the lung tissue were embedded in paraffin blocks, and sections of 10 μm were cut. The sections were stained for H&E as per standard protocol. Masson's trichrome staining was carried out using a kit (Poly Scientific, Bay Shore, New York, USA). The stained sections were examined using an Olympus microscope (Olympus Corporation, Tokyo, Japan) and photographed.

Immunohistochemical staining for α-smooth muscle actin and Mac-3

The immunohistochemical staining for α-smooth muscle actin (α-SMA) and Mac-3 was carried out on paraffin-embedded tissue. The lung sections were deparaffinized using xylene and alcohol and hydrated to water. The sections were then treated with α-SMA (Invitrogen, Carlsbad, California, USA) and Mac-3 (BD Biosciences, San Jose, California, USA) primary antibodies and incubated in a moisturized chamber for 2 h at room temperature. The sections were then washed thrice in cold PBS and incubated with biotinylated antirabbit and antimouse immunoglobulins for 30 min. The slides were washed again and treated with horseradish peroxidase-labeled streptavidin, and incubated for further 30 min. The final stain was developed using 3% 3-amino-9-ethylcarbazole in *N*,*N*-dimethylformamide. The stained sections were counterstained with Mayer's hematoxylin, treated with ammonia water, and mounted using aqueous-based mounting medium. The slides were examined under a Nikon microscope attached with a Spot RT Slider digital camera (Meyer Instruments, Houston, Texas, USA) and photographed. The infiltrated macrophages in 10 randomly selected microscopic fields were quantified using Image-Pro discovery software (Media Cybernetics).

Statistical analysis

Arithmetic mean and SD were calculated for all quantitative data. The results were statistically evaluated using two-way analysis of variance and compared with least significant difference method. Student's *t*-test were used in appropriate places to compare two sets of data. A value of P less than 0.05 was considered as significant.

Results

Monocrotaline-induced pulmonary arterial hypertension

Monocrotaline-induced PAH is an established animal model for pulmonary hypertension in rats [20,21]. We tried to induce PAH in mice using a single dosage of MCT (6 mg/100 g body weight) as in rats. However, this dose did not produce significant changes in the lung and in systolic right ventricular pressure. We then tried a single dosage of 10 mg and 30 mg/100 g body weight, which also failed to induce successful PAH in mice. Subsequently, we delivered a weekly dosage of 30 mg/100 g body weight and studied the pulmonary and cardiac changes beginning from 4 to 8 weeks. Even though this dosage produced chronic inflammatory changes in the mice, we could not yield consistent results (data not shown). Finally, we standardized our dosage to 60 mg/100 g body weight once a week for 8 consecutive weeks to induce significant and consistent pulmonary changes in mice.

Effect of monocrotaline treatment on animals

Serial administrations of MCT did not alter the animal body weight significantly. Signs of distress such as lethargy, prostration, and piloerection were present in certain animals. There was no edema formation. Some animals had labored respiration on latter stages. About 30% of the animals died within the first 3 weeks of injection. The remaining animals survived until the end of the study. Some of the animals sacrificed at 3 weeks

of the MCT administration prior to death demonstrated massive hepatic necrosis. Histopathological examination of the liver tissue at the end of the study showed only moderate necrosis. Masson's trichrome staining of the liver sections at the end of the study demonstrated deposition of mature collagen fibers between portal tract and central veins. There was intermittent occlusion of small portal veins.

Evaluation of monocrotaline-induced mouse model of pulmonary arterial hypertension

The pathogenesis of MCT-induced PAH was evaluated through right ventricular pressure measurements, histopathological evaluations as well as α-SMA staining. Figure 1a demonstrates right ventricular pressure measurements in wild-type and MMP-9 transgenic control mice and after treatment with MCT for 8 weeks. As clearly evident from the picture, the right ventricular pressure in MCT-treated wild-type mice was elevated from 25 to 60 mmHg (2.5-fold). The right ventricular pressure in MCT-treated MMP-9 transgenic mice was dramatically elevated above that seen in wild-type-treated animals to a mean value of 93 mmHg (about 3.7-fold). There was a slight increase in the right ventricular pressure in the MMP-9 transgenic control mice compared to the wild-type control. However, the difference was not significant. Figure 1b represents the quantitative mean value of the right ventricular pressure in six animals in each group. The elevated right ventricular pressure in MCT-treated wild-type and MMP-9 transgenic mice was significantly different ($P < 0.001$) compared to the respective untreated controls. Similarly, the elevated right ventricular pressure in MCT-treated MMP-9 transgenic mice was significantly different ($P < 0.001$) compared to the MCT-treated wild-type mice.

Gelatin zymography and Western blotting for matrix metalloproteinase-9

Figure 2a depicts the activity of both MMP-9 and MMP-2 in wild-type and MMP-9 transgenic control mice and after the induction of PAH. As evident from the figure, the mean MMP-9 activity was significantly increased ($P < 0.001$) in MCT-treated wild-type and MMP-9 transgenic animals compared with their respective nontreated controls. Similarly, the MMP-activity in MCT-treated MMP-9 transgenic mice was significantly higher ($P < 0.001$) compared with the MCT-treated wild-type mice. The MMP-9 activity was also higher ($P < 0.05$) in MMP-9 transgenic control mice compared to the wild-type control. Figure 2b shows the MMP-9 protein levels in wild-type and MMP-9 transgenic control mice with and without treatment with MCT. As in the case of zymography, the MMP-9 protein levels were also significantly increased ($P < 0.001$) in MCT-treated wild-type and MMP-9 transgenic mice compared to their respective nontreated controls. The MMP-9 protein level in the MCT-treated MMP-9 transgenic mice was also significantly higher ($P < 0.001$) to that of MCT-treated wild-type mice.

Fig. 1

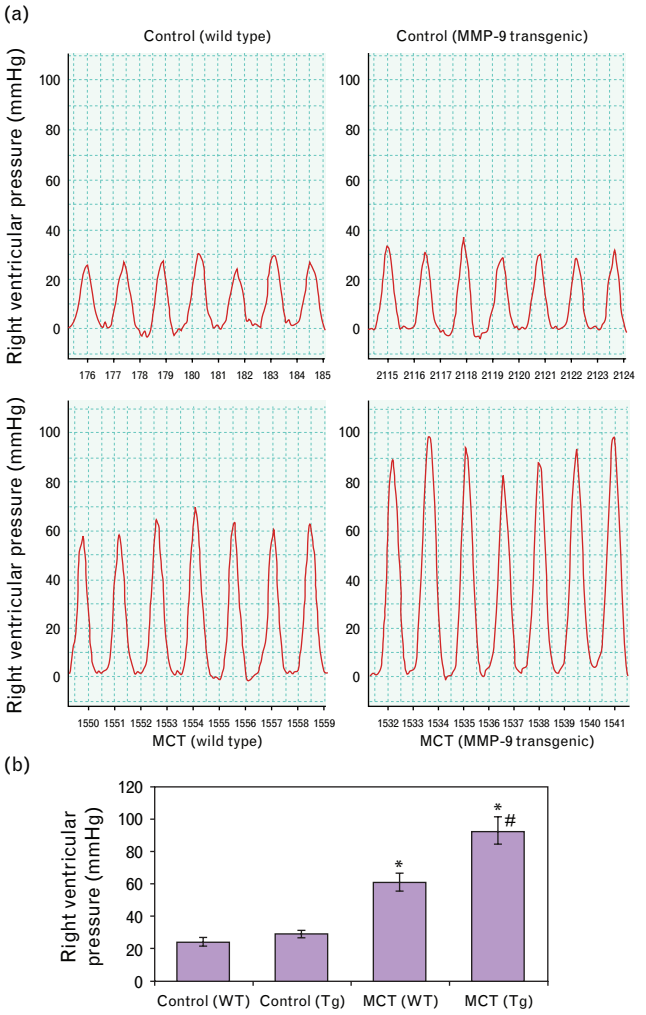

(a) Right ventricular systolic pressure measurements in wild-type and MMP-9 transgenic mice after the treatment with monocrotaline. Right ventricular pressure was measured using a 1.4F Millar Mikro-tip catheter-transducer inserted through the right jugular vein into the right atrium and to the right ventricle. MCT-induced PAH resulted in an increase of about 2.5-fold and 3.7-fold right ventricular pressure in wild-type and MMP-9 transgenic mice, respectively. The data are representative of six animals in each group. (b) Quantitative representation of right ventricular systolic pressure in wild-type and MMP-9 transgenic mice with and without MCT treatment. Data are mean ± SD of six animals in each group (*$P < 0.001$ compared with the respective untreated controls and $^{\#}P < 0.001$ compared with the MCT-treated wild-type). MCT, monocrotaline.

Real-time RT-PCR for mouse and human matrix metalloproteinase-9 mRNA expression

Figure 2c demonstrates the expression of mouse MMP-9 mRNA in wild-type and MMP-9 transgenic mice with and without treatment with MCT as well as the expression of human MMP-9 in the transgenic control and MCT-treated mice. The expression of mouse MMP-9

Fig. 2

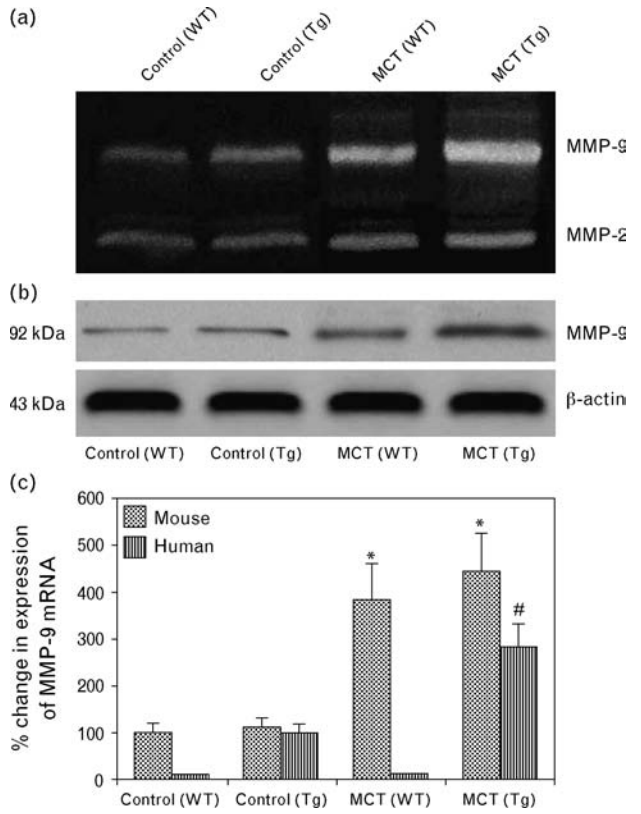

(a) Gelatin zymography for MMP-9 and MMP-2 in wild-type and MMP-9 transgenic mice with and without MCT treatment. The elevated MMP-9 activity in MCT-treated transgenic mice was contributed from both wild-type and transgenic MMP-9. (b) Western blotting for the expression of MMP-9 in the lung tissue. β-actin was used as a loading control. (c) Real-time RT-PCR analysis using SYBR green for the quantitative expression of wild-type and transgenic MMP-9 mRNA with and without MCT treatment. The data are mean ± SD of six samples ($^{*}P < 0.001$ compared with the wild-type control and $^{\#}P < 0.001$ compared with the transgenic control).

mRNA was significantly elevated ($P < 0.001$) in wild-type and transgenic mice after the treatment with MCT compared to their respective nontreated controls. Similarly, the expression of human MMP-9 mRNA was also significantly increased ($P < 0.001$) in MCT-treated transgenic mice. The increased expression of transgene in MCT-treated transgenic mice reflects the invasion of macrophages.

Hematoxylin and eosin staining

The histopathological alterations in MCT-induced PAH in wild-type and MMP-9 transgenic mice are demonstrated in Fig. 3. Figure 3a shows the normal architecture of the lung tissue in untreated wild-type mice. There was no significant alteration in the lung tissue of MMP-9 transgenic mice except the moderate infiltration of macrophages. Serial subcutaneous injections of MCT once a week for 8 consecutive weeks produced intense infiltration of mononuclear cells and macrophages in wild-type mice (Fig. 3c). The normal architecture of the alveoli has been lost in many areas. MCT administration in MMP-9 transgenic mice also resulted in dramatic infiltration of chronic inflammatory cells and macrophages into the lung parenchyma (Fig. 3d). The normal architecture of alveoli has been altered in many areas.

Masson's trichrome staining

Figure 4 demonstrates deposition of collagen fibers surrounding pulmonary vessels in MCT-induced PAH. There was no collagen deposition in both wild-type and MMP-9 transgenic untreated mice (Fig. 4a and b). However, there was extensive accumulation of collagen surrounding pulmonary vessels in the wild-type mice after the serial administrations of MCT for 8 weeks (Fig. 4c). Figure 4d depicts the marked deposition of matured collagen fibers stained in deep blue surrounding pulmonary vessels after the serial administrations of MCT in MMP-9 transgenic mice. There was extreme constriction of pulmonary vessels.

Immunohistochemical staining for α-smooth muscle actin

We carried out the immunohistochemical staining for α-SMA in order to demonstrate the proliferation and migration of smooth muscle cells and medial hypertrophy of pulmonary vessels resulting in the constriction of arteries contributing to the pathogenesis of PAH. The results of the immunohistochemical staining of α-SMA in wild-type and MMP-9 transgenic untreated mice and after the induction of PAH are presented in Fig. 5. Figure 5a depicts the α-SMA staining in a normal vessel in wild-type control mice. There was deep staining of α-SMA in MMP-9 transgenic untreated mice indicating slight thickening of the pulmonary vessels (Fig. 5b). Figure 5c and d demonstrates the α-SMA staining in wild-type mice after the induction of PAH. There was enormous staining of α-SMA in the pulmonary vessels demonstrating abnormal muscularization of distal precapillary arteries and thickening of large pulmonary arteries contributing to the development of PAH. There was complete loss of small precapillary arteries in several areas. We observed similar changes in the MMP-9 transgenic mice after the administration of MCT for 8 consecutive weeks (Fig. 5e–g). However, these changes were highly remarkable compared to the MCT-treated wild-type mice. There was progressive thickening of the wall of more proximal intra-acinar and preacinar muscular arteries with almost complete closure of large pulmonary vessels and occlusion of small vessels due to extensive proliferation and migration of smooth muscle cells, which resulted in the dramatic elevation of pulmonary arterial pressure.

Immunohistochemical staining for Mac-3

The immunohistochemical staining for Mac-3 antigen (CD 107b) in the mice lung tissue in wild-type and

Fig. 3

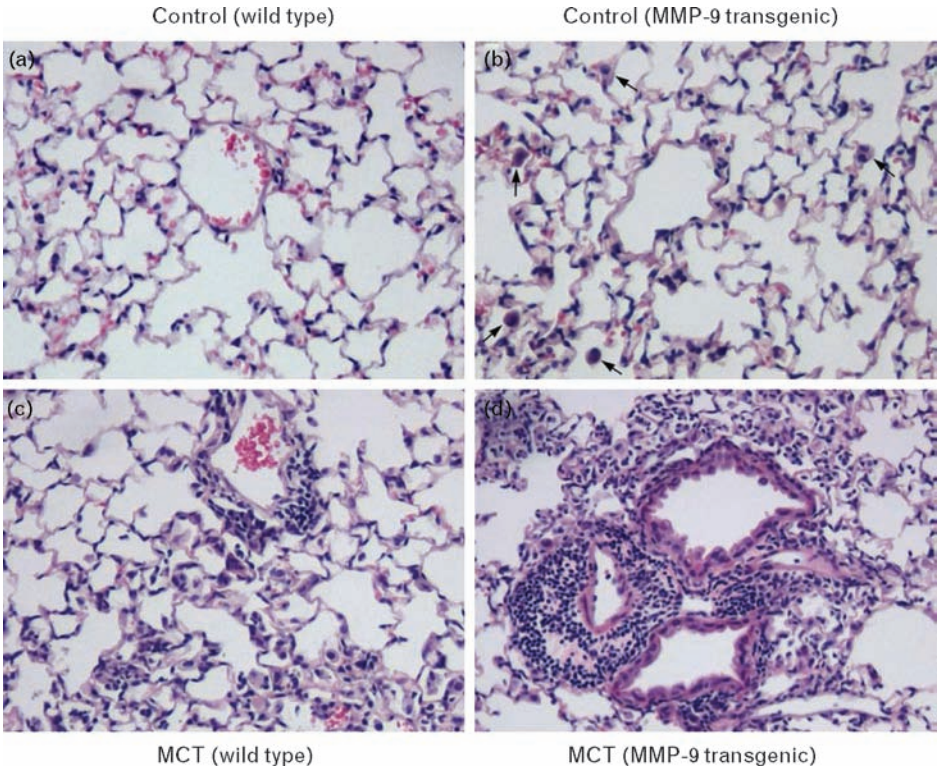

H&E staining of lung tissue in wild-type and MMP-9 transgenic mice after the treatment with monocrotaline. The data are representative of six animals in each group. (a) Wild-type mice (×100). (b) MMP-9 transgenic mice (×100). Infiltration of macrophages (arrow). (c) Wild-type mice (×100). MCT was administered in doses of 60 mg/100 g body weight once a week for 8 consecutive weeks. Loss of normal architecture of alveoli. Intense infiltration of chronic inflammatory cells. (d) MMP-9 transgenic mice (×100). MCT was administered in doses of 60 mg/100 g body weight once a week for 8 consecutive weeks. Dramatic infiltration of mononuclear inflammatory cells. Infiltration of macrophages and loss of normal architecture of alveoli. MCT, monocrotaline.

MMP-9 transgenic controls with and without treatment with MCT are demonstrated through Fig. 6a through d. The 110-kDa Mac-3 antigen is characteristic for mouse phagocytic macrophages. There was only minimal staining for Mac-3 antigen in the lung tissue of wild-type untreated mice (Fig. 6a). However, a few macrophages were present in the lung tissue of MMP-9 transgenic untreated mice (Fig. 6b). A large number of Mac-3 positive macrophages were present in the MCT administered wild-type mice indicating infiltration of macrophages (Fig. 6c). There was extensive staining for macrophages in the lung tissue of MMP-9 transgenic mice demonstrating intensive infiltration of macrophages after the treatment with MCT (Fig. 6c). Figure 6e depicts the quantitative representation of macrophages in the lung tissue. The number of infiltrated macrophages was significantly ($P < 0.001$) higher in MCT-treated wild-type and MMP-9 transgenic mice compared to their respective nontreated controls. Similarly, the number of macrophages in MCT-treated MMP-9 transgenic mice was significantly higher ($P < 0.001$) compared to the MCT-treated wild-type mice.

Discussion

This study demonstrates a reproducible animal model for PAH, which resembles the human disease. We have shown that serial subcutaneous administrations of MCT for 8 consecutive weeks could produce pulmonary arterial hypertension in mice depicting the pathophysiological features of human PAH. The MCT-induced mouse model of PAH is a reproducible and valuable animal model for studying the molecular mechanisms of the pathogenesis of PAH and may serve as an appropriate model for the rapid screening of inhibitory agents for this debilitating disease.

The most characteristic feature of PAH is the elevation of pulmonary arterial pressure. Vasoconstriction in pulmonary arteries, remodeling of the pulmonary vessel wall, and thrombosis contribute to the increased pulmonary vascular resistance in PAH [22]. An elevation of mean pulmonary arterial pressure above 25 mmHg at rest or 30 mmHg with exercise is considered as PAH [6]. An increased pulmonary arterial pressure has been reported after MCT treatment in rats [23,24] as well as in heterozygous BMPR2 mice [25].

Fig. 4

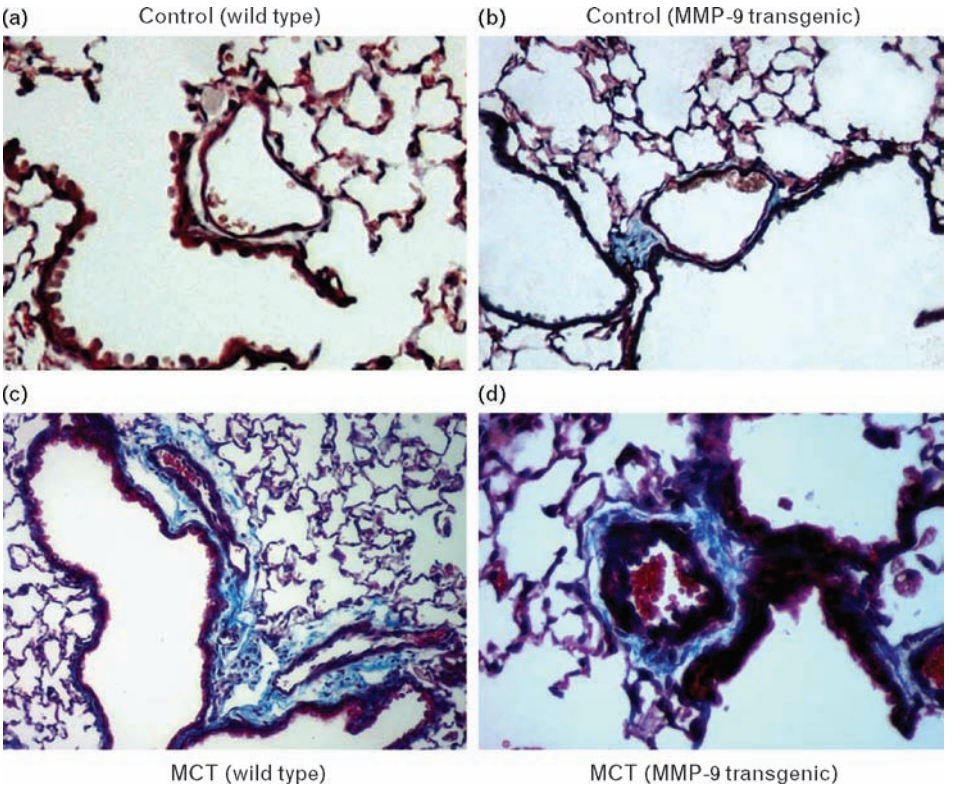

Masson's trichrome staining of lung tissue in wild-type and MMP-9 transgenic mice with and without monocrotaline treatment. The data presented are representative of six animals in each group. (a) Normal lung – wild-type mice (×200). (b) MMP-9 transgenic mice (×200). Absence of collagen deposition surrounding blood vessels. (c) MCT administered wild-type mice (×100). Marked deposition of collagen fibers stained as blue around blood vessels results in shrinkage. (d) MCT administered MMP-9 transgenic mice (×200). Intense deposition of collagen fibers surrounding blood vessels and constriction of pulmonary vessels. MCT, monocrotaline.

In this study we observed a 2.5-fold increase of pulmonary arterial pressure in wild-type and 3.7-fold increase in MMP-9 transgenic mice. The remarkable elevation of right ventricular pressure, which represents the pulmonary arterial pressure, in MMP-9 transgenic mice compared to the wild-type was due to the chronic remodeling and adventitial thickening of large pulmonary muscular arteries, occlusion of small arteries, complete loss of precapillary vessels and extensive proliferation of vascular smooth muscle cells.

The remarkable elevation of pulmonary arterial pressure in MMP-9 transgenic mice compared to the wild-type indicates that MMP-9 plays a significant role in the pathogenesis of PAH in this model system. It has been postulated that the upregulation of MMP-9 during the pathogenesis of PAH plays a crucial role in the proliferation and migration of vascular smooth muscle cells and remodeling of vascular tissue [26,27]. In this study, we have observed an increased activity and protein levels of MMP-9 as well as upregulation of MMP-9 mRNA after the administration of MCT. MMPs, especially MMP-9, play a prominent role in the degradation of extracellular matrix proteins, which facilitate the migration and proliferation of vascular smooth muscle and endothelial cells. The newly formed smooth muscle synthesizes more connective tissue components, especially interstitial collagens, which deposits surrounding the pulmonary vessels and contributes to the medial hypertrophy. The exact molecular mechanism of the upregulation of MMP-9 during the pathogenesis of PAH is not clear. Activation of signaling molecules including MAP kinases and an upregulation of MMP-9 promoter binding transcriptional factors could be responsible for the upregulation of MMP-9 [28]. The increase in smooth muscle proliferation and fibrosis in this model system is similar to that seen by our group when MMP-9 is expressed in the aneurysm of ApoE knockout mice [29].

Chronic infiltration of mononuclear cells and macrophages are characteristic features of pulmonary inflammatory process. The marked infiltration of mononuclear cells observed in this study corroborates with previous reports of MCT-induced PAH in rats [30,31]. Deposition of connective tissue components, especially mature collagen fibrils, is an inevitable phenomenon in advanced PAH [17,32]. The extensive migration and proliferation of vascular smooth muscle cells results in synthesis and

Fig. 5

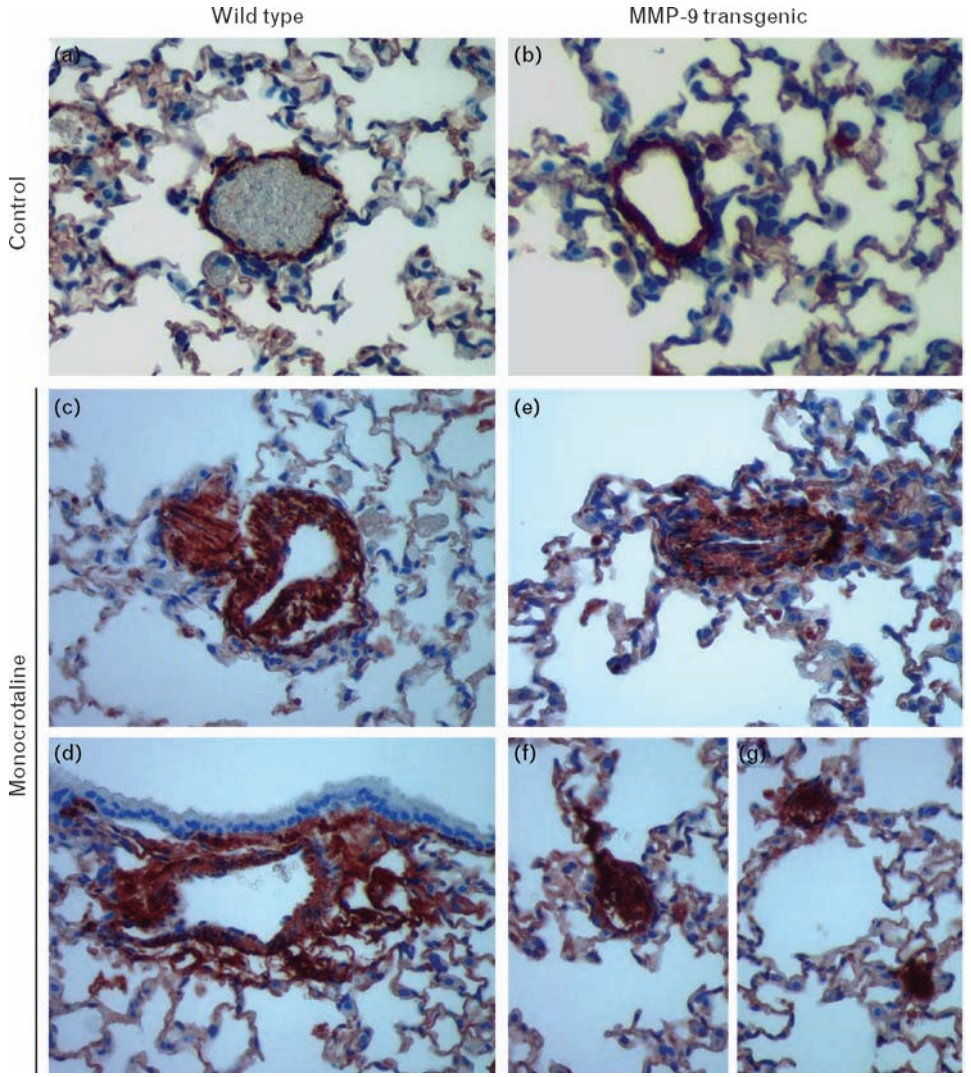

Immunohistochemical staining for α-smooth muscle actin in wild-type and MMP-9 transgenic mice with and without monocrotaline treatment. The data are representative of six animals in each group. (a) Normal lung – wild-type mice (×200). (b) MMP-9 transgenic mice (×200). A slight thickening of vessel wall by smooth muscle cells. (c and d) MCT-administered wild-type mice (×200). Extensive proliferation of smooth muscle cells and constriction of vessel walls. (e, f, and g) MCT-administered MMP-9 transgenic mice (×200). Almost complete closure of large pulmonary vessels and occlusion of small vessels due to extensive proliferation of vascular smooth muscle cells. MCT, monocrotaline.

secretion of extracellular matrix proteins, predominantly type I and type III interstitial collagens, which accumulates in the media of the pulmonary vessels. In this study, we have observed marked deposition of matured collagen fibers surrounding the pulmonary arteries, which was more prominent in MMP-9 transgenic mice, contributes to the adventitial thickening of pulmonary vessels during the pathogenesis of the PAH. Furthermore, the excessive deposition of highly crosslinked mature collagen fibrils results in the loss of intimal elasticity, which further exacerbates the situation and promotes vascular pressure.

Abnormal proliferation of endothelial and vascular smooth muscle cells within the pulmonary vascular tree is one of the most prominent features of the pathogenesis of PAH [6,33]. The normally nonmuscular peripheral arteries becomes muscular through differentiation of smooth muscle cells from precursor cells, pericytes, and intermediate cells to mature α-SMA positive smooth muscle cells [34]. The progressive thickening of the wall of proximal intra-acinar and preacinar muscular arteries and the obliteration associated with neointimal formation has been attributed to increased proliferation and migration of α-SMA positive smooth muscle cells [35]. The increase in medial wall thickness has been attributed to both hypertrophy and hyperplasia of resident smooth muscle cells and increased deposition of extracellular matrix components, especially interstitial collagens and

Fig. 6

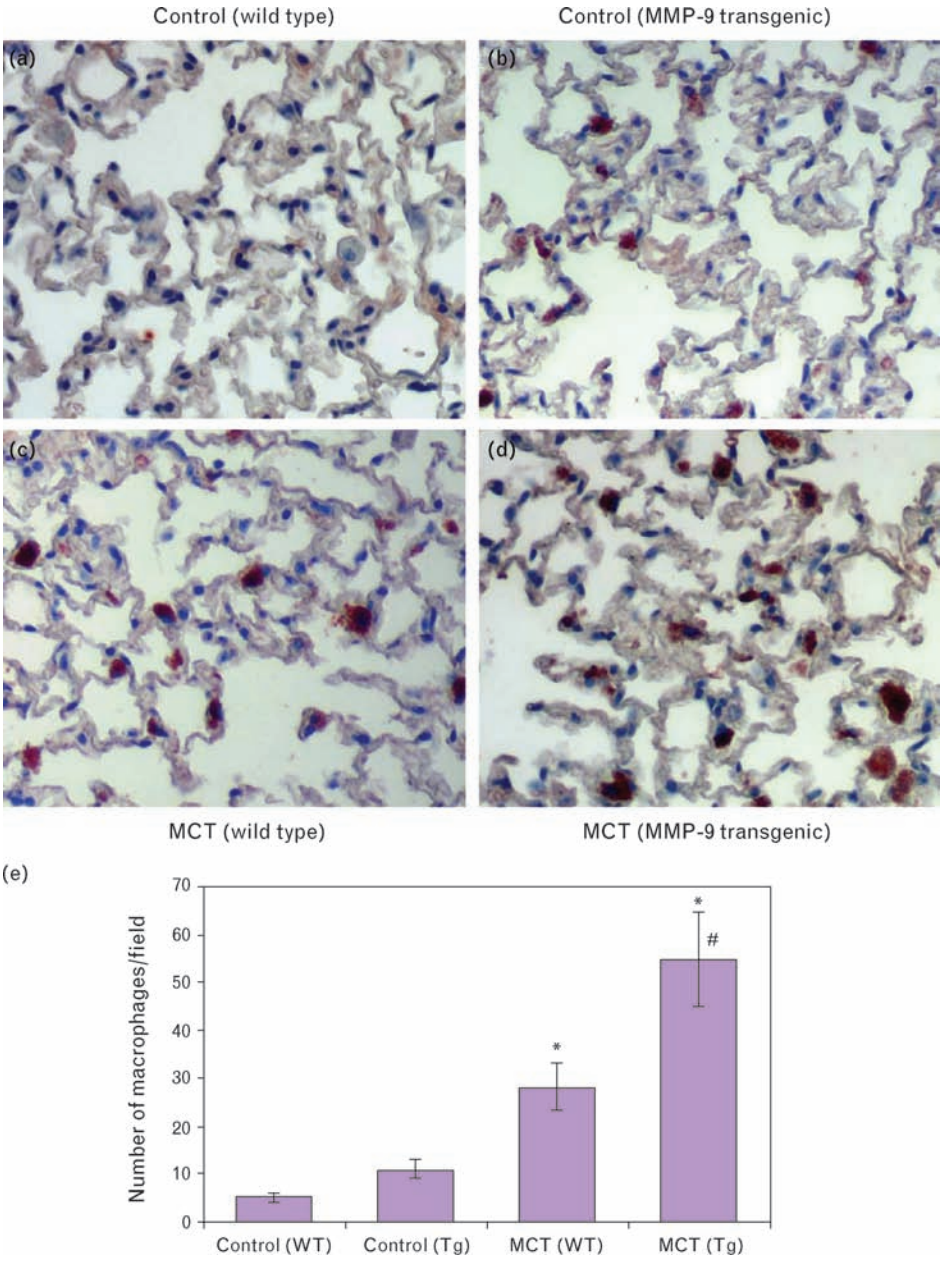

Immunohistochemical staining for Mac-3 antigen in wild-type and MMP-9 transgenic mice with and without monocrotaline treatment. The data presented are representative of six animals in each group. (a) Normal lung – wild-type mice (×200). No macrophages present. (b) MMP-9 transgenic mice (×200). Presence of few macrophages. (c) MCT-administered wild-type mice (×200). Intensive infiltration of macrophages. (d) MCT-administered MMP-9 transgenic mice (×200). Presence of large number of macrophages. (e) Quantitative representation of infiltration of macrophages. The number of macrophages in 10 randomly selected microscopic fields was quantified using Image-Pro discovery software. The data are mean ± SD of six samples ($^{*}P < 0.001$ compared with the respective untreated controls and $^{\#}P < 0.001$ compared with the MCT-treated wild-type). MCT, monocrotaline.

intercellular connective tissue, which ultimately manifest as an increase in mean pulmonary arterial pressure [36]. In this study, we have observed remarkable proliferation and migration of smooth muscle cells, deposition of collagen and occlusive arterial lesions. The pulmonary artery smooth muscle cells from patients with primary pulmonary hypertension exhibit abnormal growth responses to TGF-β1 and bone morphogenetic proteins and that the altered integration of TGF-β1 superfamily growth signals may be responsible for the abnormal proliferation and migration of smooth muscle cells and contribute to the pathogenesis of PAH [37]. Interestingly,

MMP-9 activation of TGF-β1 led to the increase in fibrosis in the atherosclerosis model previously described [29] and may be a similar mechanism by which MMP-9 is increasing fibrosis in this model system.

In conclusion, our study demonstrated that the MCT-induced mouse model of PAH is a reproducible and potent model for the human disease. Our data further identify MMP-9 as an important molecule in the pathogenesis of PAH contributing to the fibrosis and remodeling of pulmonary vessels, and effective blockade of MMP-9 could pave the way for the therapeutic intervention of this chronic disease.

Acknowledgements

This work was supported by National Institutes of Health grant HL086936 to J.D.A.

There are no conflicts of interest.

References

1 Gaine SP, Rubin LJ. Primary pulmonary hypertension. *Lancet* 1998; **352**:719–725.
2 Raiesdana A, Loscalzo J. Pulmonary arterial hypertension. *Ann Med* 2006; **38**:95–110.
3 Pietra GG, Capron F, Stewart S, Leone O, Humbert M, Robbins IM, *et al.* Pathologic assessment of vasculopathies in pulmonary hypertension. *J Am Coll Cardiol* 2004; **43**:25S–32S.
4 Theo Schermuly R, Ardeschir Ghofrani H, Weissmann N. Prostanoids and phosphodiesterase inhibitors in experimental pulmonary hypertension. *Curr Top Dev Biol* 2005; **67**:251–284.
5 Tuder RM, Marecki JC, Richter A, Fijalkowska I, Flores S. Pathology of pulmonary hypertension. *Clin Chest Med* 2007; **28**:23–42.
6 Rabinovitch M. Molecular pathogenesis of pulmonary arterial hypertension. *J Clin Invest* 2008; **118**:2372–2379.
7 Farber HW, Loscalzo J. Pulmonary arterial hypertension. *N Engl J Med* 2004; **351**:1655–1665.
8 Humbert M, Morrell NW, Archer SL, Stenmark KR, MacLean MR, Lang IM, *et al.* Cellular and molecular pathobiology of pulmonary arterial hypertension. *J Am Coll Cardiol* 2004; **43**:13S–24S.
9 Kay JM, Heath D. *Crotalaria spectabilis: the pulmonary hypertension plant*. Springfield, IL: Thomas; 1969. pp. 1–146.
10 Wilson DW, Segall HJ, Pan LC, Lamé MW, Estep JE, Morin D. Mechanisms and pathology of monocrotaline pulmonary toxicity. *Crit Rev Toxicol* 1992; **22**:307–325.
11 Rosenberg HC, Rabinovitch M. Endothelial injury and vascular reactivity in monocrotaline pulmonary hypertension. *Am J Physiol* 1988; **255**:H1484–H1491.
12 Molteni A, Ward WF, Ts'ao CH, Solliday NH. Monocrotaline pneumotoxicity in mice. *Virchows Arch B Cell Pathol Incl Mol Pathol* 1989; **57**:149–155.
13 Ohbayashi H. Matrix metalloproteinases in lung diseases. *Curr Protein Pept Sci* 2002; **3**:409–421.
14 Lagente V, Manoury B, Nénan S, Le Quément C, Martin-Chouly C, Boichot E. Role of matrix metalloproteinases in the development of airway inflammation and remodeling. *Braz J Med Biol Res* 2005; **38**:1521–1530.
15 Foronjy R, Nkyimbeng T, Wallace A, Thankachen J, Okada Y, Lemaitre V, D'Armiento J. Transgenic expression of matrix metalloproteinase-9 causes adult-onset emphysema in mice associated with the loss of alveolar elastin. *Am J Physiol Lung Cell Mol Physiol* 2008; **294**:L1149–L1157.
16 Thakker-Varia S, Tozzi CA, Poiani GJ, Babiarz JP, Tatem L, Wilson FJ, Riley DJ. Expression of matrix-degrading enzymes in pulmonary vascular remodeling in the rat. *Am J Physiol* 1998; **275**:L398–L406.
17 Novotná J, Herget J. Possible role of matrix metalloproteinases in reconstruction of peripheral pulmonary arteries induced by hypoxia. *Physiol Res* 2002; **51**:323–334.
18 Frisdal E, Gest V, Vieillard-Baron A, Levame M, Lepetit H, Eddahibi S, *et al.* Gelatinase expression in pulmonary arteries during experimental pulmonary hypertension. *Eur Respir J* 2001; **18**:838–845.
19 Snoek-van Beurden PA, Von den Hoff JW. Zymographic techniques for the analysis of matrix metalloproteinases and their inhibitors. *Biotechniques* 2005; **38**:73–83.
20 Kolettis T, Vlahos AP, Louka M, Hatzistergos KE, Baltogiannis GG, Agelaki MM, *et al.* Characterisation of a rat model of pulmonary arterial hypertension. *Hell J Cardiol* 2007; **48**:206–210.
21 Ito T, Okada T, Miyashita H, Nomoto T, Nonaka-Sarukawa M, Uchibori R, *et al.* Interleukin-10 expression mediated by an adeno-associated virus vector prevents monocrotaline-induced pulmonary arterial hypertension in rats. *Circ Res* 2007; **101**:734–741.
22 Voelkel NF, Tuder RM, Weir EK. Pathophysiology of primary pulmonary hypertension. In: Rubin L, Rich S, editors. *Primary pulmonary hypertension*. New York, NY: Marcel Dekker; 1997. pp. 83–129.
23 Abe K, Shimokawa H, Morikawa K, Uwatoku T, Oi K, Matsumoto Y, *et al.* Long-term treatment with a Rho-kinase inhibitor improves monocrotaline-induced fatal pulmonary hypertension in rats. *Circ Res* 2004; **94**:385–393.
24 Kamezaki F, Tasaki H, Yamashita K, Tsutsui M, Koide S, Nakata S, *et al.* Gene transfer of extracellular superoxide dismutase ameliorates pulmonary hypertension in rats. *Am J Respir Crit Care Med* 2008; **177**:219–226.
25 Song Y, Coleman L, Shi J, Beppu H, Sato K, Walsh K, *et al.* Inflammation, endothelial injury, and persistent pulmonary hypertension in heterozygous BMPR2-mutant mice. *Am J Physiol Heart Circ Physiol* 2008; **295**:H677–H690.
26 Lepetit H, Eddahibi S, Fadel E, Frisdal E, Munaut C, Noel A, *et al.* Smooth muscle cell matrix metalloproteinases in idiopathic pulmonary arterial hypertension. *Eur Respir J* 2005; **25**:834–842.
27 Cantini-Salignac C, Lartaud I, Schrijen F, Atkinson J, Chabot F. Metalloproteinase-9 in circulating monocytes in pulmonary hypertension. *Fundam Clin Pharmacol* 2006; **20**:405–410.
28 Umar S, Hessel M, Steendijk P, Bax W, Schutte C, Schalij M, *et al.* Activation of signaling molecules and matrix metalloproteinases in right ventricular myocardium of rats with pulmonary hypertension. *Pathol Res Pract* 2007; **203**:863–872.
29 Lemaître V, Kim HE, Forney-Prescott M, Okada Y, D'Armiento J. Transgenic expression of matrix metalloproteinase-9 modulates collagen deposition in a mouse model of atherosclerosis. *Atherosclerosis* 2009; **205**:107–112.
30 Iwasaki T, Takahashi T, Shimizu H, Ohmori E, Morimoto T, Kajiya M, *et al.* Increased pulmonary heme oxygenase-1 and delta-aminolevulinate synthase expression in monocrotaline-induced pulmonary hypertension. *Curr Neurovasc Res* 2005; **2**:133–139.
31 White RJ, Meoli DF, Swarthout RF, Kallop DY, Galaria II, Harvey JL, *et al.* Plexiform-like lesions and increased tissue factor expression in a rat model of severe pulmonary arterial hypertension. *Am J Physiol Lung Cell Mol Physiol* 2007; **293**:L583–L590.
32 Lee KM, Tsai KY, Wang N, Ingber DE. Extracellular matrix and pulmonary hypertension: control of vascular smooth muscle cell contractility. *Am J Physiol* 1998; **274**:H76–H82.
33 Jeffery TK, Morrell NW. Molecular and cellular basis of pulmonary vascular remodeling in pulmonary hypertension. *Prog Cardiovasc Dis* 2002; **45**:173–202.
34 Rabinovitch M. Pathobiology of pulmonary hypertension. *Ann Rev Pathol Mech Dis* 2002; **2**:369–399.
35 Jones PL, Cowan KN, Rabinovitch M. Tenascin-C, proliferation and subendothelial fibronectin in progressive pulmonary vascular disease. *Am J Pathol* 1997; **150**:1349–1360.
36 Merklinger S. The pathobiology of pulmonary hypertension: lessons from experimental studies. In: Redington AN, Van Arsdell GS, Anderson RH, editors. *Congenital diseases in the right heart*. London: Springer; 2009. pp. 39–47.
37 Morrell NW, Yang X, Upton PD, Jourdan KB, Morgan N, Sheares KK, Trembath RC. Altered growth responses of pulmonary artery smooth muscle cells from patients with primary pulmonary hypertension to transforming growth factor-β1 and bone morphogenetic proteins. *Circulation* 2001; **104**:790–795.